J. Phase Equilib. Diffus. (2022) 43:483–494
https://doi.org/10.1007/s11669-022-00987-0

Quasi-Ternary System Ag_2Se–$GeSe_2$–As_2Se_3

I. A. Ivashchenko[1] · O. S. Klymovych[2] · I. D. Olekseyuk[1] · L. D. Gulay[3] · V. V. Halyan[4] · O. M. Strok[1]

Submitted: 25 October 2021 / in revised form: 30 July 2022 / Accepted: 2 August 2022 / Published online: 7 September 2022

Abstract Phase equilibria in the quasi-ternary system Ag_2Se–$GeSe_2$–As_2Se_3 were investigated by direct synthesis, x-ray phase, differential thermal and microstructural analysis methods. Isothermal section of the system at 513 K (240 °C) was constructed, the existence of ternary compounds Ag_8GeSe_6, Ag_3AsSe_3, $AgAsSe_2$, $AgAs_3Se_5$ was confirmed, and the existence of quaternary compounds was not found. Three quasi-binary phase diagrams Ag_2Se–As_2Se_3, Ag_8GeSe_6–$AgAsSe_2$, $GeSe_2$–$AgAsSe_2$, three vertical sections Ag_8GeSe_6–Ag_3AsSe_3, Ag_8GeSe_6–As_2Se_3, $GeSe_2$–$AgAs_3Se_5$, and the liquidus surface projection onto the concentration triangle were constructed. The regions of primary crystallization of phases, character, temperature, and coordinates of mono- and invariant equilibria were determined.

Keywords chalcogenides · isothermal section · liquidus surface projection · microstructural analysis · phase equilibria · thermal analysis · x-ray powder diffraction

✉ I. A. Ivashchenko
Ivashchenko.inna@vnu.edu.ua

[1] Department of Chemistry and Technology, Lesya Ukrainka Volyn National University, Lutsk, Ukraine

[2] Volyn Scientific Research Forensic Center of the MIA of Ukraine, Lutsk, Ukraine

[3] Department of Ecology and Protection of Environment, Lesya Ukrainka Volyn National University, Lutsk, Ukraine

[4] Department of Experimental Physics, Information and Education Technologies, Lesya Ukrainka Volyn National University, Lutsk, Ukraine

1 Introduction

The binary compounds Ag_2Se, $GeSe_2$, As_2Se_3 melt congruently at 1170 K (897 °C), 1013 K (740 °C), and 648 K (375 °C)[1], respectively, possess insignificant homogeneity regions and may serve as components of the quasi-ternary system Ag_2Se–$GeSe_2$–As_2Se_3. The study of this quasi-ternary system is of current interest because it is formed by binary compounds with important semiconducting properties. Complex chalcogenide semiconductors attract growing interest in materials science due to their prospects for use as materials in the fields of nonlinear optics, optoelectronics, and acousto-optics.[2-6]

Phase equilibria in the quasi-binary system Ag_2Se–$GeSe_2$ were studied in Ref 7-10. The authors of Ref 10 confirmed the existence of one ternary compound Ag_8GeSe_6 which melts congruently at 1175 K (902 °C) and undergoes two polymorphous transformations at 269 K (–4 °C)[7] and 321 K (48 °C),[7,9,10] respectively. The eutectic points coordinates were ascertained as 1103 K (830 °C), 15 mol.% $GeSe_2$ and 843 K (570 °C), 56 mol.% $GeSe_2$,[10] and agree well with Ref 7. γ-Ag_8GeSe_6 which is stable at room temperature crystallizes in space group, S.G. $Pmn2_1$, with lattice parameters a = 0.7823 nm, b = 0.7712 nm, c = 1.0885 nm.[11]

The Ag_2Se–As_2Se_3 phase diagram was described in Ref 12-14. According to Ref 14, the existence of three compounds, Ag_3AsSe_3, $AgAsSe_2$ and $AgAs_3Se_5$, was established in the system. The $AgAs_3Se_5$ compound forms incongruently at 643 K (370 °C) and has a eutectic with As_2Se_3 at 87 mol.% As_2Se_3 and 630 K (357 °C). The $AgAsSe_2$ compound melts congruently at 673 K (400 °C) and does not have a polymorphous transformation (whereas according to Ref 13 there is a polymorphous transformation of $AgAsSe_2$ at 658 K (385 °C)). The peritectic reaction $L + Ag_2Se \leftrightarrow Ag_3AsSe_3$ takes place at 663 K

(390 °C). The coordinates of the eutectic of Ag_3AsSe_3 – $AgAsSe_2$ are 33 mol.% As_2Se_3 and 653 K (380 °C).

The crystal structure of the Ag_3AsSe_3 compound was determined in Ref 13, 15. The compound is an analogue of the proustite mineral (Ag_3AsS_3), crystallizes in S.G. $R3c$; and has lattice parameters a = 1.1285 nm, c = 0.8803 nm [13], or a = 1. 1298 nm, c = 0.8757 nm[15]. For the high-temperature modification (HTM) of $AgAsSe_2$, the authors of Ref 13 determined the crystal structure S.G. $R\ \bar{3}\ m$, structure type $NaCrS_2$, a = 0.3915 nm, c = 2.0375 nm. The diffraction pattern of the low-temperature modification (LTM) of $AgAsSe_2$ was indexed by the authors of Ref 13 in the primitive tetragonal cell with a = 1.2548 nm, c = 1.1140 nm. The compound $AgAs_3Se_5$ crystallizes in S.G. $R\ \bar{3}\ m$, a = 0.38195(1) nm, c = 5.0082(2) nm[16].

Phase diagram of the $GeSe_2$–As_2Se_3 system of the eutectic type, with the eutectic point at 20 mol.% $GeSe_2$ and 618 K (345 °C)[17].

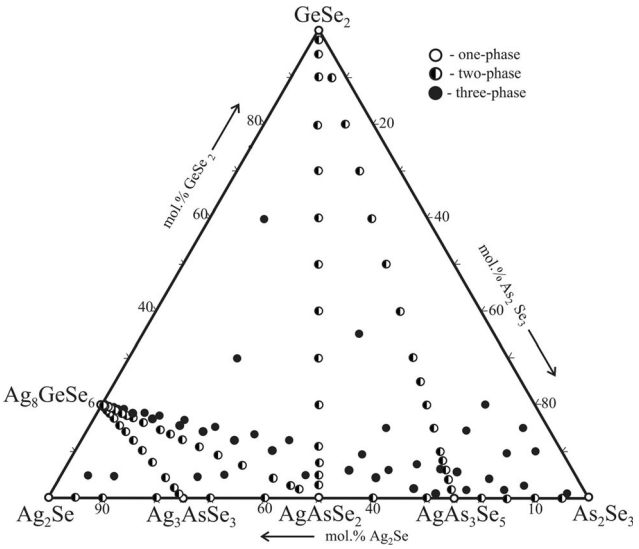

Fig. 1 Chemical and phase compositions of the Ag_2Se–$GeSe_2$–As_2Se_3 system samples at 513 K

2 Experimental Methods

Phase equilibria in the quasi-ternary system Ag_2Se–$GeSe_2$–As_2Se_3 were studied using 122 samples. The alloys were synthesized by direct single-temperature method from high-purity elements (Ag 99.995, Ge 99.99, Se 99.9997, As 99.9999 wt.%) in quartz containers that were evacuated to a residual pressure of 0.133 Pa and sealed. The synthesis was performed in a shaft-type furnace with temperature control with an accuracy of ± 5 K (± 5 °C). The maximum synthesis temperature was 1373 K (1100 °C), the heating and cooling rate was 10 K/h (10 °C/h). Homogenization annealing at 513 K (240 °C) was held for 600 h, after which the samples were quenched into 25% aqueous NaCl solution.

The as-obtained samples were investigated by x-ray diffraction (XRD) method (DRON 4–13 diffractometer, CuK_α radiation, $10(20)° < 2\theta < 90°$, 0.05° scan step, 1–5 s exposure in each point) and differential thermal analysis (DTA) ("Thermodent H307/1" furnace with a PDA-1 XY-recorder, Pt/Pt–Rh thermocouple). The two-phase or three-phase composition of the samples was also checked by the microstructure analysis (MSA), which was performed on a PMT-3 M microhardness tester.

3 Results and Discussion

3.1 *Isothermal Section of the Quasi-Ternary System Ag_2Se–$GeSe_2$–As_2Se_3 at 513 K (240 °C)*

According to XRD and MSA results of 122 samples (Fig. 1), isothermal section of the Ag_2Se – $GeSe_2$ – As_2Se_3 system at 513 K was plotted (Fig. 2). Diffraction patterns of the binary compounds were indexed (Fig. 3): $GeSe_2$ by S.G. $P2_1/c$, a = 0.7007(2) nm, b = 1.6819(5) nm, c = 1.1806(3) nm, β = 90.74(2)°; As_2Se_3 in S.G. $P2_1/n$, a = 1.2794(7) nm, b = 0.9874(5) nm, c = 0.4267(2) nm, α = 90.96(4)°, and agree well with the literature data from Ref 18-20, respectively. The existence of the four ternary compounds Ag_8GeSe_6, Ag_3AsSe_3, LTM-$AgAsSe_2$, $AgAs_3Se_5$ was confirmed (Fig. 3). The diffraction pattern of the Ag_8GeSe_6 compound was indexed with the orthorhombic S.G. $Pmn2_1$, a = 0.78443(5) nm, b = 0.77372(5) nm, c = 1.09141(7) nm, which is consistent with Ref 11. The diffraction pattern of Ag_3AsSe_3 was

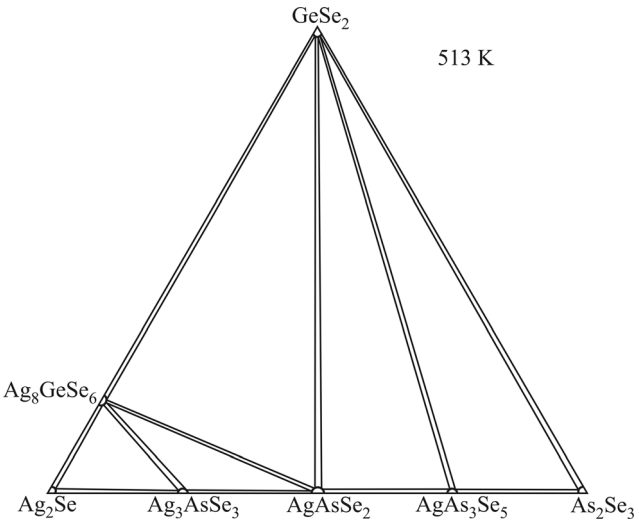

Fig. 2 Isothermal section of the quasi-ternary system Ag_2Se–$GeSe_2$–As_2Se_3 at 513 K

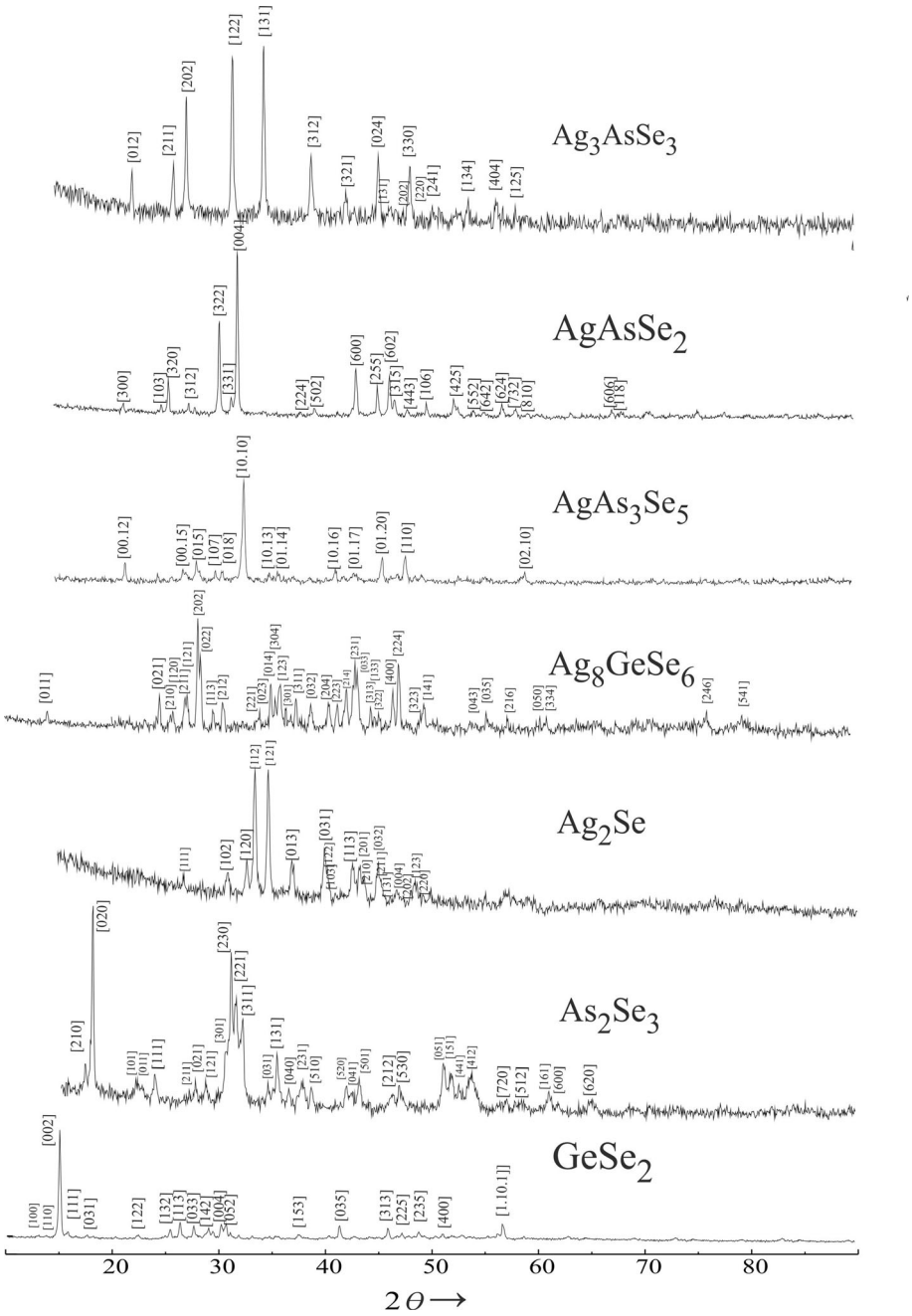

Fig. 3 Experimental diffractograms of the binary and ternary compounds of the quasi-ternary system Ag_2Se–$GeSe_2$–As_2Se_3

indexed with the hexagonal S.G. *R*3*c*, structural type proustite Ag_3AsS_3, a = 1.1270(6) nm, c = 0.8765(9) nm, which agrees with Ref 13. The LTM-$AgAsSe_2$ was identified by comparing our diffraction pattern with the one indexed with a tetragonal structure (a = 1.2548 nm, c = 1.1140 nm) presented in Ref 13. The crystal structure of the $AgAs_3Se_5$ compound was determined by the powder diffraction method. It was found that the compound crystallizes in S.G. $R\ \bar{3}\ m$, a 0.38195(1) nm, c = 5.0082(2) nm)[16]. Ag_2Se was obtained as a LTM (S.G. $P2_12_12_1$, a = 0.4337(5) nm, b = 0.7072(5) nm, c = 0.7773(5) nm).

The presence of the four two-phase equilibria, Ag_8GeSe_6–Ag_3AsSe_3, Ag_8GeSe_6–$AgAsSe_2$ (Fig. 4), $GeSe_2$–$AgAsSe_2$, and $GeSe_2$–$AgAs_3Se_5$, was established in the studied quasi-ternary system according to x-ray phase analysis and MSA of the synthesized samples. They divide the system into the respective regions of three-phase equilibria $Ag_2Se + Ag_8GeSe_6 + Ag_3AsSe_3$, $Ag_3AsSe_3 + Ag_8GeSe_6 + AgAsSe_2$, $AgAsSe_2 + Ag_8GeSe_6 + GeSe_2$, $AgAs_3Se_5 + AgAsSe_2 + GeSe_2$ and $As_2Se_3 + AgAs_3Se_5 + GeSe_2$. No significant solid solubility ranges were found for the binary compounds or intermediate ternary compounds.

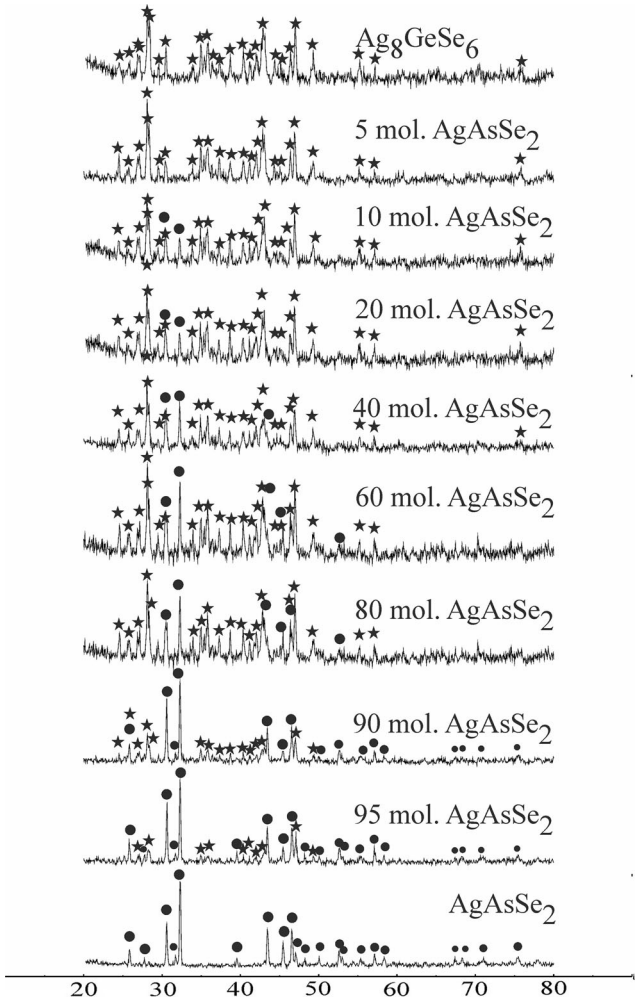

Fig. 4 Experimental diffractograms of the samples of the Ag_8GeSe_6–$AgAsSe_2$ system (compositions are given in mol.%)

3.2 *The Quasi-Binary System Ag_2Se–As_2Se_3*

Due to somewhat differing literature data in Ref 12-14, we re-investigated the Ag_2Se–As_2Se_3 system (Fig. 5). The compositions of the samples for the investigation are given in Table 1. Phase diagram of the system was plotted from the results of XRD, DTA (Table 1) and MSA. The existence and formation mechanism of three compounds Ag_3AsSe_3, $AgAsSe_2$ and $AgAs_3Se_5$, and the polymorphous transformation of $AgAsSe_2$ were confirmed. Ag_3AsSe_3 melts incongruently at 660 K (387 °C), $AgAsSe_2$ melts congruently at 683 K (410 °C), and $AgAs_3Se_5$ melts incongruently at 644 K (371 °C). The horizontal line at 635 K (362 °C) corresponds to the eutectic reaction $L_{e1} \leftrightarrow AgAs_3Se_5 + As_2Se_3$ with the eutectic point at 88 mol.% As_2Se_3. The temperatures of invariant reactions practically do not differ from Ref 15. The phase diagram of the Ag_2Se – As_2Se_3 system shows a horizontal line at 630 K (357 °C) which indicates a polymorphous

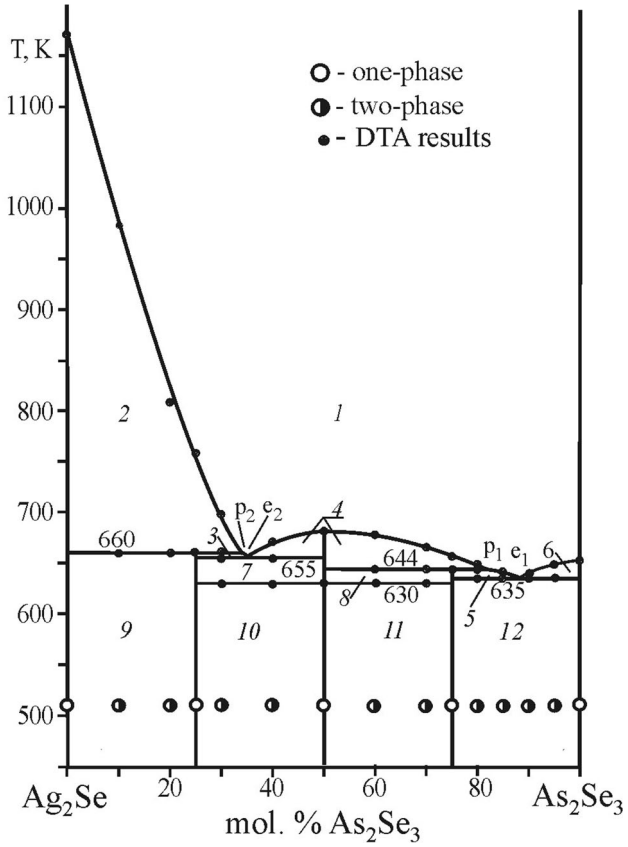

Fig. 5 Phase diagram of the Ag_2Se–As_2Se_3 system: 1–L; 2–L + Ag_2Se, 3–L + Ag_3AsSe_3, 4–L + HTM-$AgAsSe_2$, 5–L + $AgAs_3Se_5$, 6–L + As_2Se_3, 7–Ag_3AsSe_3 + HTM-$AgAsSe_2$, 8–HTM-$AgAsSe_2$ + $AgAs_3Se_5$, 9–Ag_2Se + Ag_3AsSe_3, 10–Ag_3AsSe_3 + LTM-$AgAsSe_2$, 11–LTM-$AgAsSe_2$ + $AgAs_3Se_5$, 12–$AgAs_3Se_5$ + As_2Se_3

transformation of the $AgAsSe_2$ compound; obtained temperature value is slightly lower than indicated in Ref 12, 13.

3.3 *The Quasi-Binary System Ag_8GeSe_6–$AgAsSe_2$*

Phase diagram of the Ag_8GeSe_6 – $AgAsSe_2$ system (Fig. 6) is based on DTA, XRD and MSA results. The axes of the isothermal section (Fig. 1 and 2) and the liquidus projection (Fig. 12) are in mol.% of the components, Ag_2Se, As_2Se_3 and $GeSe_2$, while the axes of the vertical sections (Figs. 6-11) are in mol.% of the compounds constituting these sections. For easier correlation with the isothermal section and the liquidus projection, a secondary axis with mol.% of As_2Se_3 is added to the diagram. The compositions of the synthesized samples as well as DTA results are given in Table 2. Some of the DTA curves are shown in Fig. 7. They were measured from and till the temperature of annealing of the samples, 513 K. The investigated system is of the eutectic type. The eutectic point coordinates

Table 1 Compositions of the samples of the Ag_2Se–As_2Se_3 quasi-binary system and their DTA results

No.	Composition, mol. %	T, K
1	Ag_2Se	**1170**
2	90 Ag_2Se–10 As_2Se_3	**983**; 660
3	80 Ag_2Se–20 As_2Se_3	**810**; 660
4	75 Ag_2Se–25 As_2Se_3	**757**; 660
5	70 Ag_2Se–30 As_2Se_3	**697**; 660; 655; 630
6	60 Ag_2Se–40 As_2Se_3	**670**; 655; 630
7	50 Ag_2Se–50 As_2Se_3	**683**; 630
8	40 Ag_2Se–60 As_2Se_3	**675**; 644; 630
9	30 Ag_2Se–70 As_2Se_3	**665**; 644; 630
10	25 Ag_2Se–75 As_2Se_3	**657**; 644
11	20 Ag_2Se–80 As_2Se_3	**650**; 644; 635
12	15 Ag_2Se–85 As_2Se_3	**642**; 635
13	10 Ag_2Se–90 As_2Se_3	**640**; 635
14	5 Ag_2Se–95 As_2Se_3	**648**; 635
15	As_2Se_3	**652**

Bold values indicate the melting temperatures of the samples

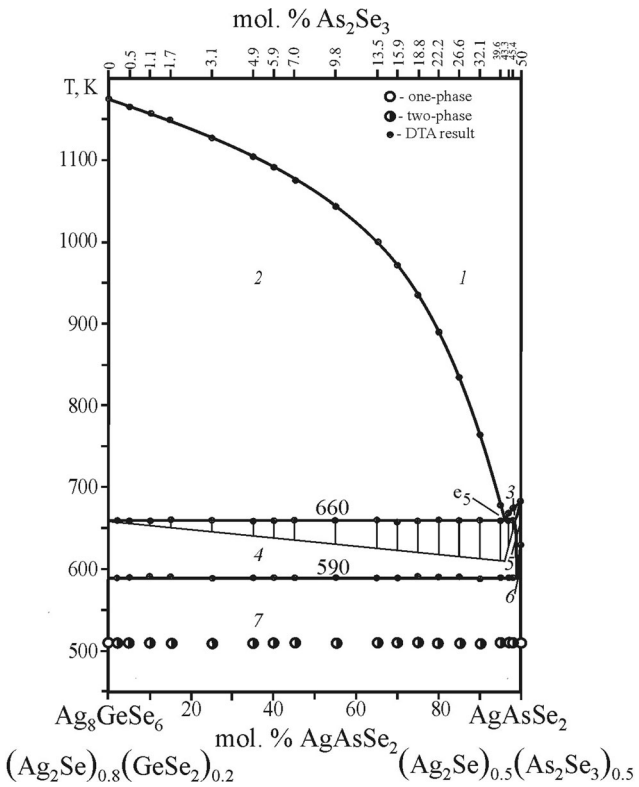

Fig. 6 Phase diagram of the Ag_8GeSe_6–$AgAsSe_2$ system: 1–L, 2–L + Ag_8GeSe_6, 3–L + HTM-$AgAsSe_2$, 4–Ag_8GeSe_6 + HTM-$AgAsSe_2$, 5–HTM-$AgAsSe_2$, 6–HTM-$AgAsSe_2$ + LTM-$AgAsSe_2$, 7–Ag_8GeSe_6 + LTM-$AgAsSe_2$

Table 2 Compositions of the samples of the Ag_8GeSe_6–$AgAsSe_2$ quasi-binary system calculated through the ternary, binary compounds and their DTA results

No.	Composition, mol. %	T, K
1	Ag_8GeSe_6	**1175**
	(80 Ag_2Se–20 $GeSe_2$–0 As_2Se_3)	
2	98 Ag_8GeSe_6–2 $AgAsSe_2$	-; 660; 590
	(79.9 Ag_2Se–19.9 $GeSe_2$–0.2 As_2Se_3)	
3	95 Ag_8GeSe_6–5 $AgAsSe_2$	**1165**; 659; 591
	(79.7 Ag_2Se–19.8 $GeSe_2$–0.5 As_2Se_3)	
4	90 Ag_8GeSe_6–10 $AgAsSe_2$	**1160**; 659; 592
	(79.3 Ag_2Se–19.6 $GeSe_2$–1.1 As_2Se_3)	
5	85 Ag_8GeSe_6–15 $AgAsSe_2$	**1150**; 661; 592
	(79.0 Ag_2Se–19.3 $GeSe_2$–1.7 As_2Se_3)	
6	75 Ag_8GeSe_6–25 $AgAsSe_2$	**1125**; 660; 590
	(78.1 Ag_2Se–18.8 $GeSe_2$–3.1 As_2Se_3)	
7	65 Ag_8GeSe_6–35 $AgAsSe_2$	**1105**; 659; 590
	(77.1 Ag_2Se–18.1 $GeSe_2$–4.9 As_2Se_3)	
8	60 Ag_8GeSe_6–40 $AgAsSe_2$	**1090**; 660; 590
	(76.5 Ag_2Se–17.6 $GeSe_2$–5.9 As_2Se_3)	
9	55 Ag_8GeSe_6–45 $AgAsSe_2$	**1075**; 660; 590
	(75.8 Ag_2Se–17.2 $GeSe_2$–7.0 As_2Se_3)	
10	45 Ag_8GeSe_6–55 $AgAsSe_2$	**1020**; 660; 591
	(74.1 Ag_2Se–16.1 $GeSe_2$–9.8 As_2Se_3)	
11	35 Ag_8GeSe_6–65 $AgAsSe_2$	**1000**; 661; 590
	(71.9 Ag_2Se–14.6 $GeSe_2$–13.5 As_2Se_3)	
12	30 Ag_8GeSe_6–70 $AgAsSe_2$	**970**; 659; 590
	(70.5 Ag_2Se–13.6 $GeSe_2$–15.9 As_2Se_3)	
13	25 Ag_8GeSe_6–75 $AgAsSe_2$	**935**; 660; 592
	(68.8 Ag_2Se–12.5 $GeSe_2$–18.8 As_2Se_3)	
14	20 Ag_8GeSe_6–80 $AgAsSe_2$	**890**; 661; 591
	(66.7 Ag_2Se–11.1 $GeSe_2$–22.2 As_2Se_3)	
15	15 Ag_8GeSe_6–85 $AgAsSe_2$	**840**; 660; 592
	(64.1 Ag_2Se–9.4 $GeSe_2$–26.6 As_2Se_3)	
16	10 Ag_8GeSe_6–90 $AgAsSe_2$	**765**; 660; 588
	(60.7 Ag_2Se–7.1 $GeSe_2$–32.1 As_2Se_3)	
17	5 Ag_8GeSe_6–95 $AgAsSe_2$	**680**; 660; 590
	(56.3 Ag_2Se–4.2 $GeSe_2$–39.6 As_2Se_3)	
18	3 Ag_8GeSe_6–97 $AgAsSe_2$	**670**; 660; 590
	(54.02 Ag_2Se–2.68 $GeSe_2$–43.30 As_2Se_3)	
19	2 Ag_8GeSe_6–98 $AgAsSe_2$	**675**; 660; 590
	(52.8 Ag_2Se–1.9 $GeSe_2$–45.4 As_2Se_3)	
20	$AgAsSe_2$	**683**; 630
	(50.0 Ag_2Se–0 $GeSe_2$–50.0 As_2Se_3)	

Bold values indicate the melting temperatures of the samples

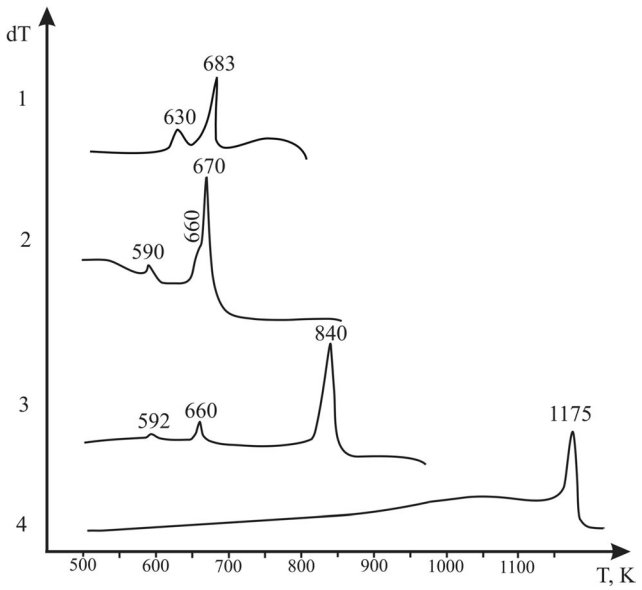

Fig. 7 DTA curves of some alloys of the Ag_8GeSe_6–$AgAsSe_2$ system: 1–$AgAsSe_2$, 2–97 mol.% $AgAsSe_2$ − 3 mol.% Ag_8GeSe_6, 3–85 mol.% $AgAsSe_2$ − 15 mol.% Ag_8GeSe_6, 4–Ag_8GeSe_6

were determined by plotting the Tammann triangle according to Ref 21. Point e_5 corresponds to the composition of 4 mol.% Ag_8GeSe_6–96 mol.% $AgAsSe_2$ (55.2 mol.% Ag_2Se–3.4 mol.% $GeSe_2$–41.4 mol.% As_2Se_3), 660 K (387 °C), where the invariant reaction $L_{e5} \leftrightarrow Ag_8GeSe_6 + HTM\text{-}AgAsSe_2$ takes place. The liquidus is represented by the curves of the primary crystallization of Ag_8GeSe_6 and the solid solution HTM-$AgAsSe_2$. The eutectoid reaction HTM-$AgAsSe_2 \leftrightarrow$ LTM-$AgAsSe + Ag_8GeSe_6$ takes place at 590 K (317 °C). Below this temperature the samples are two-phase, Ag_8GeSe_6 + LTM-$AgAsSe_2$, which was established by XRD (Fig. 4) and MSA methods. No significant solid solubility based on the starting compounds was observed.

3.4 *The Vertical Section Ag_8GeSe_6–Ag_3AsSe_3*

The compositions and DTA data of the alloys are given in Table 3. Based on these the vertical section was built. The liquidus (Fig. 8) crosses the primary crystallization regions of Ag_8GeSe_6 (field 2) and Ag_2Se (field 4). The regions of the secondary crystallization of the monovariant eutectic reaction $L_{e3\text{-}U1} \leftrightarrow Ag_2Se + Ag_8GeSe_6$ (field 3) and the peritectic reaction $L_{p2\text{-}U1} + Ag_2Se \leftrightarrow Ag_3AsSe_3$ (field 5) descend to the plane of the invariant reaction $L_{U1} + Ag_2Se \leftrightarrow Ag_8GeSe_6 + Ag_3AsSe_3$ which occurs at 650 K (377 °C) and ends with the exhaustion of L and Ag_2Se. Therefore, below 650 K (377 °C) the samples are two-phase $Ag_8GeSe_6 + Ag_3AsSe_3$ (field 6), which was determined by XRD and MSA data. No solid solubility based on the starting compounds was found.

Table 3 Compositions of the samples of the Ag_8GeSe_6 – Ag_3AsSe_3 vertical section calculated from the compositions of the ternary, binary compounds and their DTA results

No	Composition. mol. %	T, K
1	Ag8GeSe6	**1175**
	(80 Ag2Se–20 GeSe2–0 As2Se3)	
2	98 Ag8GeSe6–2 Ag3AsSe3	**1170**; 965; 649
	(79.96 Ag2Se–19.84 GeSe2–0.20 As2Se3)	
3	95 Ag8GeSe6–5 Ag3AsSe3	**1162**; 964; 649
	(79.90 Ag2Se–19.59 GeSe2–0.52 As2Se3)	
4	90 Ag8GeSe6–10 Ag3AsSe3	**1150**; 963; 650
	(79.79 Ag2Se–19.15 GeSe2–1.06 As2Se3)	
5	80 Ag8GeSe6–20 Ag3AsSe3	**1126**; 963; 649
	(79.55 Ag2Se–18.18 GeSe2–2.27 As2Se3)	
6	70 Ag8GeSe6–30 Ag3AsSe3	**1105**; 964; 650
	(79.27 Ag2Se–17.07 GeSe2–3.66 As2Se3)	
7	60 Ag8GeSe6–40 Ag3AsSe3	**1080**; 963; 650
	(78.95 Ag2Se–15.79 GeSe2–5.26 As2Se3)	
8	50 Ag8GeSe6–50 Ag3AsSe3	**1162**; 965; 650
	(78.57 Ag2Se–14.29 GeSe2–7.14 As2Se3)	
9	40 Ag8GeSe6–60 Ag3AsSe3	**1040**; 964; 650
	(78.13 Ag2Se–12.50 GeSe2–9.38 As2Se3)	
10	30 Ag8GeSe6–70 Ag3AsSe3	**1010**; 964; 650
	(77.59 Ag2Se–10.34 GeSe2–12.07 As2Se3)	
11	20 Ag8GeSe6–80 Ag3AsSe3	**964**; 650
	(76.92 Ag2Se–7.96 GeSe2–15.38 As2Se3)	
12	10 Ag8GeSe6–90 Ag3AsSe3	**925**; 785; 650
	(76.09 Ag2Se–4.35 GeSe2–19.57 As2Se3)	
13	5 Ag8GeSe6–95 Ag3AsSe3	**882**; 650
	(75.58 Ag2Se–2.33 GeSe2–22.09 As2Se3)	
14	2 Ag8GeSe6–98 Ag3AsSe3	**805**; 650
	(75.24 Ag2Se–0.97 GeSe2–23.79 As2Se3)	
15	Ag3AsSe3	**757**; 660
	(75 Ag2Se–0 GeSe2–25 As2Se3)	

Bold values indicate the melting temperatures of the samples

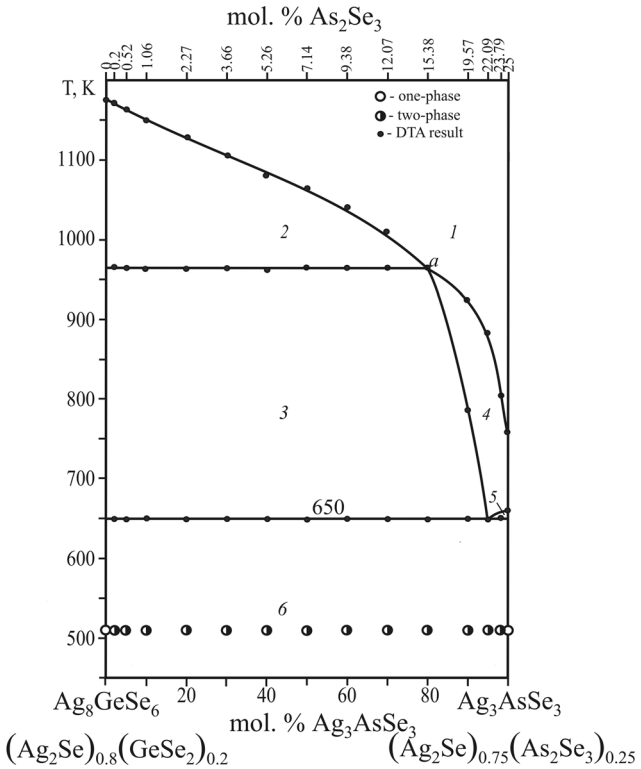

Fig. 8 The vertical section Ag_8GeSe_6–Ag_3AsSe_3: 1–L, 2–L + Ag_8GeSe_6, 3–L + Ag_2Se + Ag_8GeSe_6, 4–L + Ag_2Se, 5–L + Ag_2Se + Ag_3AsSe_3, 6–Ag_8GeSe_6 + Ag_3AsSe_3

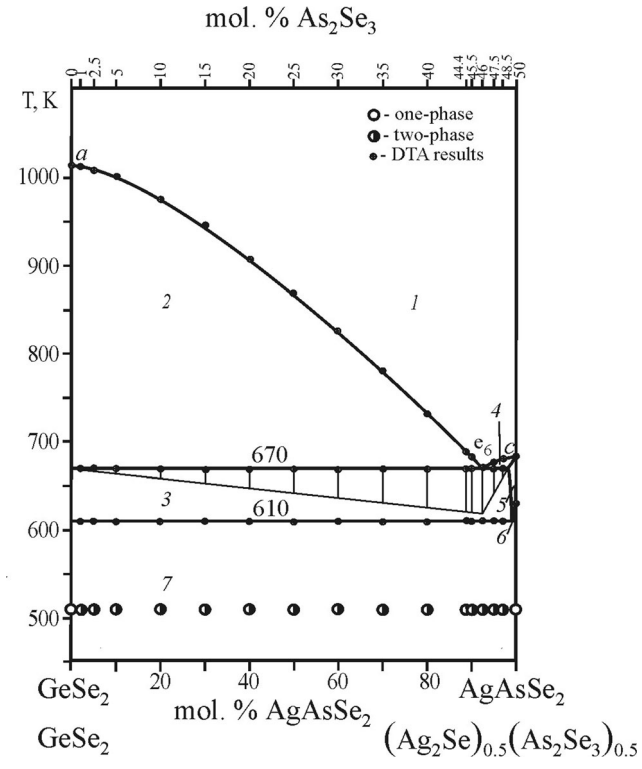

Fig. 9 Phase diagram of the $GeSe_2$–$AgAsSe_2$ system: 1–L, 2–L + $GeSe_2$, 3–$GeSe_2$ + HTM-$AgAsSe_2$, 4–L + HTM-$AgAsSe_2$, 5–HTM-$AgAsSe_2$, 6–HTM-$AgAsSe_2$ + LTM-$AgAsSe_2$, 7–$GeSe_2$ + LTM-$AgAsSe_2$

3.5 *The Quasi-Binary System $GeSe_2$ – $AgAsSe_2$*

Phase diagram of the $GeSe_2$–$AgAsSe_2$ system (Fig. 9) is based on DTA (Table 4), XRD and MSA results for 16 samples, compositions of which are given in Table 4. Phase diagram is of the eutectic type, the liquidus consists of the curves of the primary crystallization of $GeSe_2$ (*ab*) and the solid solution HTM-$AgAsSe_2$ (*bc*), respectively. The horizontal line at 670 K (397 °C) corresponds to the invariant eutectic reaction $L_{e6} \leftrightarrow GeSe_2 + \text{HTM-}AgAsSe_2$. The coordinates of the eutectic point e_6 are 7.7 mol.% $GeSe_2$–92.3 mol.% $AgAsSe_2$ (46 mol.% Ag_2Se–8 mol.% $GeSe_2$–46 mol.% As_2Se_3) as determined by plotting the Tammann triangle. The eutectoid reaction HTM-$AgAsSe_2 \leftrightarrow$ LTM-$AgAsSe_2 + GeSe_2$ takes place at 610 K (337 °C). Below this temperature, the samples are two-phase $GeSe_2$ + LTM-$AgAsSe_2$ that is consistent with Fig. 2. No significant solid solubility based on the starting compounds was detected.

3.6 *The Vertical Section Ag_8GeSe_6–As_2Se_3*

The Ag_8GeSe_6 – As_2Se_3 section (Fig. 10) is based on XRD, MSA and DTA results of 20 samples. Their compositions and DTA data are shown in Table 5. The liquidus of the vertical section is represented by the primary crystallization curves of Ag_8GeSe_6 (*ab*), $GeSe_2$ (*bcd*), HTM-$AgAsSe_2$ (*df*), $AgAs_3Se_5$ (*fg*) and As_2Se_3 (*gj*). The section crosses two subsystems of the studied quasi-ternary system, $AgAsSe_2 + Ag_8GeSe_6 + GeSe_2$ (II) and $AgAsSe_2$ + $GeSe_2 + As_2Se_3$ (III). The section crosses the plane of the invariant eutectic reaction $L_{E2} \leftrightarrow$ HTM-$AgAsSe_2$ + $Ag_8GeSe_6 + AgAs_3Se_5$ at 630 K (357 °C) in subsystem II. This ends with the exhaustion of liquid, therefore the alloys are three-phase (field 12) below 630 K (357 °C) in the region between 2 and 75 mol.% As_2Se_3. The horizontal at 590 K (317 °C) represents the reaction HTM-$AgAsSe_2 \leftrightarrow$ LTM-$AgAsSe_2 + Ag_8GeSe_6 + GeSe_2$ in the subsolidus region, and alloys below 590 K contain LTM-$AgAsSe_2$ and are three-phase (LTM-$AgAsSe_2 + Ag_8GeSe_6 + GeSe_2$).

Table 4 Compositions of the samples of the $GeSe_2$–$AgAsSe_2$ quasi-binary system calculated from the compositions of the ternary, binary compounds and their DTA results

No	Composition, mol. %	T, K
1	$GeSe_2$	**1013**
2	98 $GeSe_2$–2 $AgAsSe_2$ (Ag_2Se–98 $GeSe_2$–As_2Se_3)	**1011**; 670; 610
3	95 $GeSe_2$–5 $AgAsSe_2$ (2.5 Ag_2Se–95 $GeSe_2$–2.5 As_2Se_3)	**1007**; 671; 610
4	90 $GeSe_2$–10 $AgAsSe_2$ (5 Ag_2Se–90 $GeSe_2$–5 As_2Se_3)	**1002**; 670; 609
5	80 $GeSe_2$–20 $AgAsSe_2$ (10 Ag_2Se–80 $GeSe_2$–10 As_2Se_3)	**975**; 670; 610
6	70 $GeSe_2$–30 $AgAsSe_2$ (15 Ag_2Se–70 $GeSe_2$–15 As_2Se_3)	**949**; 669; 610
7	60 $GeSe_2$–40 $AgAsSe_2$ (20 Ag_2Se–60 $GeSe_2$–20 As_2Se_3)	**907**; 669; 610
8	50 $GeSe_2$–50 $AgAsSe_2$ (25 Ag_2Se–50 $GeSe_2$–25 As_2Se_3)	**868**; 669; 609
9	40 $GeSe_2$–60 $AgAsSe_2$ (30 Ag_2Se–40 $GeSe_2$–30 As_2Se_3)	**825**; 669; 610
10	30 $GeSe_2$–70 $AgAsSe_2$ (35 Ag_2Se–30 $GeSe_2$–35 As_2Se_3)	**780**; 670; 610
11	20 $GeSe_2$–80 $AgAsSe_2$ (40 Ag_2Se–20 $GeSe_2$–40 As_2Se_3)	**730**; 670; 610
12	11.2 $GeSe_2$–88.8 $AgAsSe_2$ (44.4 Ag_2Se–11.2 $GeSe_2$–44.4 As_2Se_3)	**690**; 670; 610
13	9 $GeSe_2$–91 $AgAsSe_2$ (45.5 Ag_2Se–9 $GeSe_2$–45.5 As_2Se_3)	**683**; 670; 609
14	8 $GeSe_2$–92 $AgAsSe_2$ (46 Ag_2Se–8 $GeSe_2$–46 As_2Se_3)	**670**; 610
15	5 $GeSe_2$–95 $AgAsSe_2$ (47.5 Ag_2Se–5 $GeSe_2$–47.5 As_2Se_3)	**676**; 670; 610
16	3 $GeSe_2$–97 $AgAsSe_2$ (48.5 Ag_2Se–3 $GeSe_2$–48.5 As_2Se_3)	**680**; 670; 610
17	$AgAsSe_2$ (50 Ag_2Se–0 $GeSe_2$–50 As_2Se_3)	**683**; 630

Bold values indicate the melting temperatures of the samples

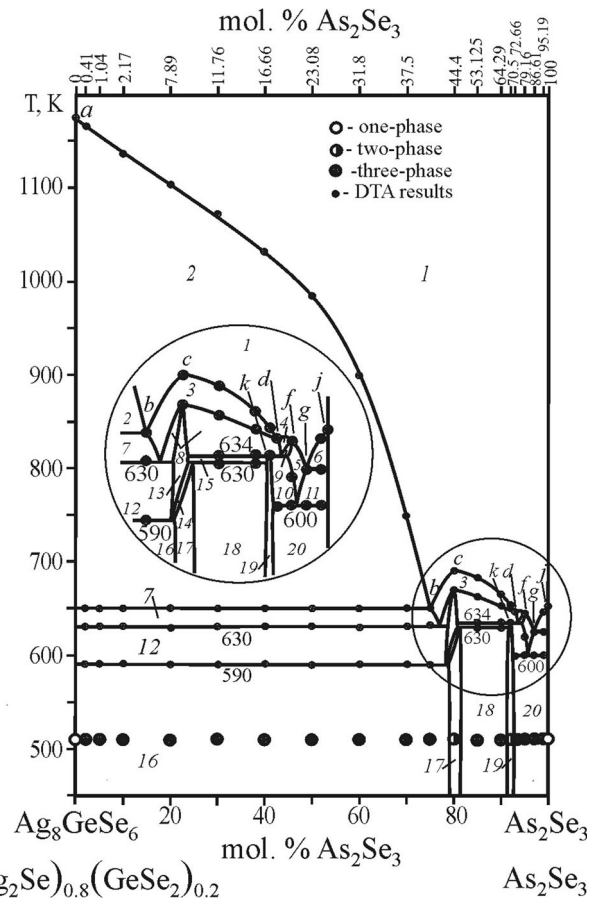

Fig. 10 The vertical section Ag_8GeSe_6–As_2Se_3: 1–L, 2–L + Ag_8GeSe_6, 3–L + $GeSe_2$, 4–L + HTM-$AgAsSe_2$, 5–L + $AgAs_3Se_5$, 6–L + As_2Se_3, 7–L + Ag_8GeSe_6 + $GeSe_2$, 8–L + HTM-$AgAsSe_2$ + $GeSe_2$, 9–L + HTM-$AgAsSe_2$ + $AgAs_3Se_5$, 10–L + $GeSe_2$ + $AgAs_3Se_5$, 11–L + $AgAs_3Se_5$ + As_2Se_3, 12–Ag_8GeSe_6 + HTM-$AgAsSe_2$ + $GeSe_2$, 13–$GeSe_2$ + HTM-$AgAsSe_2$, 14–$GeSe_2$ + HTM-$AgAsSe_2$ + LTM-$AgAsSe_2$, 15–HTM-$AgAsSe_2$ + $GeSe_2$ + $AgAs_3Se_5$, 16–Ag_8GeSe_6 + LTM-$AgAsSe_2$ + $GeSe_2$, 17–$GeSe_2$ + LTM-$AgAsSe_2$, 18–LTM-$AgAsSe_2$ + $GeSe_2$ + $AgAs_3Se_5$, 19–$GeSe_2$ + $AgAs_3Se_5$, 20–$GeSe_2$ + $AgAs_3Se_5$ + As_2Se_3

The sample with 80 mol.% As_2Se_3 is two-phase at the annealing temperature (LTM-$AgAsSe_2$ + $GeSe_2$) because it falls on the quasi-binary section $GeSe_2$–$AgAsSe_2$. The section in subsystem III crosses the reaction plane at 634 K (361 °C) which reflects the invariant reaction L_{U2} + HTM-$AgAsSe_2$ ↔ $AgAs_3Se_5$ + $GeSe_2$. This reaction ends in samples with higher Ag_8GeSe_6 content with the disappearance of the liquid, so that the alloys of this subsystem below 634 K (361 °C) are three-phase (field 15). The horizontal line at 630 K (357 °C) corresponds to the reaction HTM-$AgAsSe_2$ + $AgAs_3Se_5$ ↔ LTM-$AgAsSe_2$ + $GeSe_2$ in the subsolidus region, thus the alloys below 630 K (357 °C) contain LTM-$AgAsSe_2$ and are three-phase ($AgAs_3Se_5$ + LTM-$AgAsSe_2$ + $GeSe_2$). This reaction ends in point *k* with the exhaustion of both L and HTM-$AgAsSe_2$, so that the alloys are two-phase $GeSe_2$ + $AgAs_3Se_5$ below 630 K (357 °C) (field 19). Samples with higher As_2Se_3 content end in the invariant reaction at 634 K (361 °C) with the exhaustion of HTM-$AgAsSe_2$. Therefore, the alloys below 634 K (361 °C) are three-phase L + $GeSe_2$ + $AgAs_3Se_5$ (field 10). This field together with the region of the secondary crystallization L + As_2Se_3 + $AgAs_3Se_5$ (field 11) descends to the plane

Table 5 Compositions of the samples of the Ag_8GeSe_6 – As_2Se_3 vertical section calculated from the compositions of the ternary, binary compounds and their DTA results

No	Composition, mol. %	T, K
1	Ag_8GeSe_6	**1175**
	(80 Ag_2Se–20 $GeSe_2$–0 As_2Se_3)	
2	98 Ag_8GeSe_6–2 As_2Se_3	**1165**; 650; 630; 590
	(79.67 Ag_2Se–19.92 $GeSe_2$–0.41 As_2Se_3)	
3	95 Ag_8GeSe_6–5 As_2Se_3	-; 650; 630; 590
	(79.17 Ag_2Se–19.79 $GeSe_2$–1.04 As_2Se_3)	
4	90 Ag_8GeSe_6–10 As_2Se_3	**1135**; 650; 630; 591
	(78.26 Ag_2Se–19.57 $GeSe_2$–2.17 As_2Se_3)	
5	80 Ag_8GeSe_6–20 As_2Se_3	**1100**; 650; 629; 590
	(76.19 Ag_2Se–19.05 $GeSe_2$–4.76 As_2Se_3)	
6	70 Ag_8GeSe_6–30 As_2Se_3	**1070**; 650; 630; 590
	(73.68 Ag_2Se–18.43 $GeSe_2$–7.89 As_2Se_3)	
7	60 Ag_8GeSe_6–40 As_2Se_3	**1030**; 650; 630; 591
	(70.59 Ag_2Se–17.65 GeSe–11.76 As_2Se_3)	
8	50 Ag_8GeSe_6–50 As_2Se_3	**985**; 650; 630; 589
	(66.67 Ag_2Se–16.67 $GeSe_2$–16.66 As_2Se_3)	
9	40 Ag_8GeSe_6–60 As_2Se_3	**900**; 650; 630; 590
	(61.54 Ag_2Se–15.38 $GeSe_2$–23.08 As_2Se_3)	
10	30 Ag_8GeSe_6–70 As_2Se_3	**750**; 650; 630; 590
	(54.54 Ag_2Se–13.64 $GeSe_2$–31.82 As_2Se_3)	
11	25 Ag_8GeSe_6–75 As_2Se_3	**650**; 631; 590
	(50 Ag_2Se–12.5 $GeSe_2$–37.5 As_2Se_3)	
12	20 Ag_8GeSe_6–80 As_2Se_3	**690**; 670; -
	(44.4 Ag_2Se–11.2 $GeSe_2$–44.4 As_2Se_3)	
13	15 Ag_8GeSe_6–85 As_2Se_3	**682**; 663; 634; 630
	(37.5 Ag_2Se–9.375 $GeSe_2$–53.125 As_2Se_3)	
14	10 Ag_8GeSe_6–90 As_2Se_3	**665**; 652; 634; 630
	(28.57 Ag_2Se–7.14 $GeSe_2$–64.29 As_2Se_3)	
15	7.7 Ag_8GeSe_6–92.3 As_2Se_3	**653**; -; 634
	(23.5 Ag_2Se–6 $GeSe_2$–70.5 As_2Se_3)	
16	7 Ag_8GeSe_6–93 As_2Se_3	**645**; -; 600
	(21.87 Ag_2Se–5.47 $GeSe_2$–72.66 As_2Se_3)	
17	5 Ag_8GeSe_6–95 As_2Se_3	**644**; 620; 600
	(16.67 Ag_2Se–4.17 $GeSe_2$–79.16 As_2Se_3)	
18	3 Ag_8GeSe_6–97 As_2Se_3	**625**; 600
	(10.71 Ag_2Se–2.68 $GeSe_2$–86.61 As_2Se_3)	
19	1 Ag_8GeSe_6–99 As_2Se_3	**645**; 625; 600
	(3.85 Ag_2Se–0.96 $GeSe_2$–95.19 As_2Se_3)	
20	As_2Se_3	**652**

Bold values indicate the melting temperatures of the samples

of the invariant reaction $L_{E3} \leftrightarrow GeSe_2 + As_2Se_3 + AgAs_3Se_5$ at 600 K (327 °C). This reaction ends with the exhaustion of the liquid; thus, the alloys are three-phase ($GeSe_2 + As_2Se_3 + AgAs_3Se_5$) below 600 K (327 °C). This agrees with the results shown in Fig. 2. The phase composition of the samples was determined by XRD and MSA results.

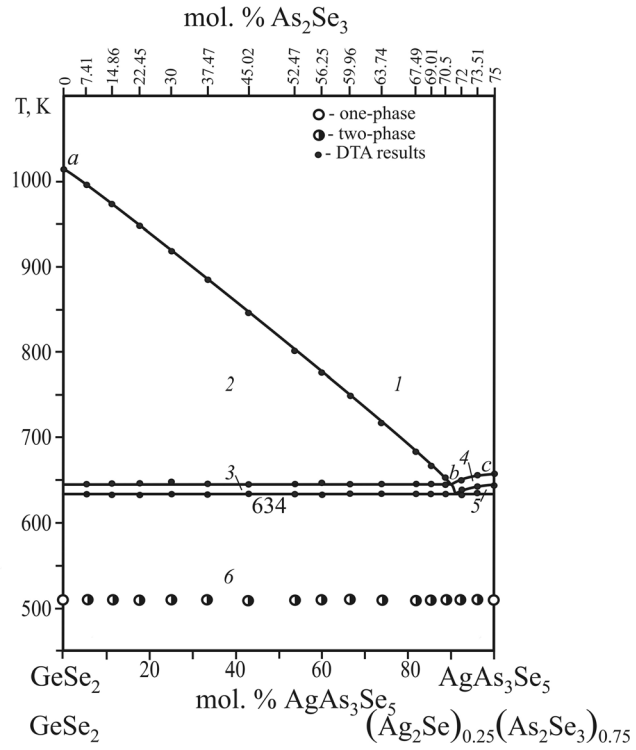

Fig. 11 The vertical section $GeSe_2$–$AgAs_3Se_5$: 1–L, 2–L + $GeSe_2$, 3–L + HTM-$AgAsSe_2$ + $GeSe_2$, 4–L + HTM-$AgAsSe_2$, 5–L + HTM-$AgAsSe_2$ + $AgAs_3Se_5$, 6–$GeSe_2$–$AgAs_3Se_5$

3.7 *The Vertical Section $GeSe_2$ – $AgAs_3Se_5$*

The section (Fig. 11) was investigated by DTA, XRD and MSA of 17 samples with compositions given in Table 6. The liquidus consists of the curves of the primary crystallization of $GeSe_2$ (*ab*) and HTM-$AgAsSe_2$ (*bc*). The section crosses the plane of the invariant reaction L_{U2} + HTM-$AgAsSe_2 \leftrightarrow AgAs_3Se_5 + GeSe_2$ at 634 K (361 °C), which ends with the exhaustion of both L and HTM-$AgAsSe_2$, so that the alloys are two-phase below 634 K (361 °C) as confirmed by XRD and MSA results.

3.8 *Liquidus Surface Projection of the Quasi-Ternary System Ag_2Se–$GeSe_2$–As_2Se_3*

The liquidus surface projection of the quasi-ternary system Ag_2Se–$GeSe_2$–As_2Se_3 (Fig. 12 and Table 7) is based on literature data and our own results from studies of three phase diagrams Ag_2Se–As_2Se_3, Ag_8GeSe_6–$AgAsSe_2$ and $GeSe_2$–$AgAsSe_2$ and three vertical sections Ag_8GeSe_6–Ag_3AsSe_3, Ag_8GeSe_6–As_2Se_3 and $GeSe_2$–$AgAs_3Se_5$, as well as the isothermal section of the system at 513 K (240 °C).

Table 6 Compositions of the samples of the $GeSe_2$–$AgAs_3Se_5$ vertical section calculated from the compositions of the ternary, binary compounds and their DTA results

No	Composition, mol. %	T, K
1	$GeSe_2$	**1013**
2	94.8 $GeSe_2$–5.2 $AgAs_3Se_5$ (2.47 Ag_2Se–90.11 $GeSe_2$–7.41 As_2Se_3)	**995**; 645; 634
3	89 $GeSe_2$–11 $AgAs_3Se_5$ (4.95 Ag_2Se–80.18 $GeSe_2$–14.86 As_2Se_3)	**973**; 646; 633
4	82.4 $GeSe_2$–17.6 $AgAs_3Se_5$ (7.48 Ag_2Se–70.07 $GeSe_2$–22.45 As_2Se_3)	**947**; 647; 633
5	75 $GeSe_2$–25 $AgAs_3Se_5$ (10 Ag_2Se–60 $GeSe_2$–30 As_2Se_3)	**917**; 648; 634
6	66.7 $GeSe_2$–33.3 $AgAs_3Se_5$ (12.49 Ag_2Se–50.04 $GeSe_2$–37.47 As_2Se_3)	**885**; 645; 634
7	57.2 $GeSe_2$–42.8 $AgAs_3Se_5$ (14.97 Ag_2Se–40.01 $GeSe_2$–45.02 As_2Se_3)	**845**; 645; 634
8	46.2 $GeSe_2$–53.8 $AgAs_3Se_5$ (17.49 Ag_2Se–30.04 $GeSe_2$–52.47 As_2Se_3)	**801**; 645; 634
9	40 $GeSe_2$–60 $AgAs_3Se_5$ (18.75 Ag_2Se–25 $GeSe_2$–56.25 As_2Se_3)	**775**; 646; 633
10	33.4 $GeSe_2$–66.6 $AgAs_3Se_5$ (19.99 Ag_2Se–20.05 $GeSe_2$–59.96 As_2Se_3)	**750**; 645; 634
11	26.1 $GeSe_2$–73.9 $AgAs_3Se_5$ (21.25 Ag_2Se–15.01 $GeSe_2$–63.74 As_2Se_3)	**717**; 645; 634
12	18.2 $GeSe_2$–81.8 $AgAs_3Se_5$ (22.5 Ag_2Se–10.01 $GeSe_2$–67.49 As_2Se_3)	**683**; 645; 634
13	14.8 $GeSe_2$–85.2 $AgAs_3Se_5$ (23.0 Ag_2Se–7.99 $GeSe_2$–69.01 As_2Se_3)	**667**; 645; 634
14	11.3 $GeSe_2$–88.7 $AgAs_3Se_5$ (23.5 Ag_2Se–6 $GeSe_2$–70.5 As_2Se_3)	**653**; 645; 634
15	7.7 $GeSe_2$–92.3 $AgAs_3Se_5$ (24 Ag_2Se–4 $GeSe_2$–72 As_2Se_3)	**650**; 638; 634
16	3.9 $GeSe_2$–96.1 $AgAs_3Se_5$ (24.5 Ag_2Se–1.99 $GeSe_2$–73.51 As_2Se_3)	**655**; 642; 635
17	$AgAs_3Se_5$ (25 Ag_2Se–75 As_2Se_3)	**657**; 644

Bold values indicate the melting temperatures of the samples

The system's liquidus consists of the fields of the primary crystallization of Ag_2Se (Ag_2Se-p_2-U_1-e_3-Ag_2Se), Ag_3AsSe_3 (e_2-E_1-U_1-p_2-e_2), HTM-$AgAsSe_2$ (p_1-U_2-e_6-E_2-e_5-E_1-e_2-p_1), $AgAs_3Se_5$ (e_1-E_3-U_2-p_1-e_1), As_2Se_3 (As_2Se_3-e_7-E_3-e_1-As_2Se_3), Ag_8GeSe_6 (e_3-U_1-E_1-e_5-E_2-e_4-e_3) and $GeSe_2$ ($GeSe_2$-e_7-E_3-U_2-e_6-E_2-e_4-$GeSe_2$). The largest fields correspond to the primary crystallization of Ag_8GeSe_6 and $GeSe_2$. The fields of the primary crystallization are

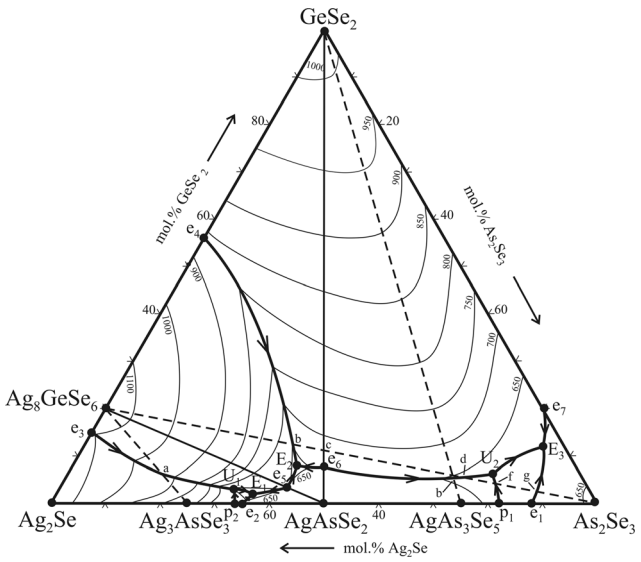

Fig. 12 Liquidus surface projection of the quasi-ternary system Ag_2Se–$GeSe_2$–As_2Se_3

separated by 13 monovariant curves of binary eutectic and peritectic reactions and 14 invariant points (Table 7).

The system undergoes five quaternary invariant reactions (Table 7): transition $L_{U1} + Ag_2Se \leftrightarrow Ag_8GeSe_6 + Ag_3AsSe_3$ at 650 K (377 °C), eutectic $L_{E1} \leftrightarrow Ag_8GeSe_6 + Ag_3AsSe_3 + HTM\text{-}AgAsSe_2$ at 640 K (367 °C), eutectic $L_{E2} \leftrightarrow Ag_8GeSe_6 + GeSe_2 + HTM\text{-}AgAsSe_2$ at 630 K (357 °C), transition $L_{U2} + HTM\text{-}AgAsSe_2 \leftrightarrow AgAs_3Se_5 + GeSe_2$ at 634 K (361 °C) and eutectic $L_{E3} \leftrightarrow GeSe_2 + As_2Se_3 + AgAs_3Se_5$ at 600 K (327 °C).

4 Conclusions and Future Work

Phase equilibria in the Ag_2Se–$GeSe_2$–As_2Se_3 system were investigated for the first time by XRD and MSA. At 513 K (240 °C) four ternary compounds Ag_8GeSe_6, Ag_3AsSe_3, $AgAsSe_2$, $AgAs_3Se_5$ were identified and an isothermal section of Ag_2Se–$GeSe_2$–As_2Se_3 system was constructed. The liquidus surface projection of the quasi-ternary system Ag_2Se–$GeSe_2$–As_2Se_3 was plotted according to the investigation of the vertical sections Ag_8GeSe_6–Ag_3AsSe_3, Ag_8GeSe_6–As_2Se_3, $GeSe_2$–$AgAs_3Se_5$ and phase diagrams Ag_2Se–As_2Se_3, Ag_8GeSe_6–$AgAsSe_2$, $GeSe_2$ – $AgAsSe_2$. There are seven fields of the primary crystallization of Ag_2Se, Ag_3AsSe_3, HTM-$AgAsSe_2$, $AgAs_3Se_5$, As_2Se_3, Ag_8GeSe_6 and $GeSe_2$ on the liquidus surface projection with the largest fields of Ag_8GeSe_6 and $GeSe_2$ compounds. In the investigated system there are two transition reactions: $L_{U1} + Ag_2Se \leftrightarrow Ag_8GeSe_6 + Ag_3AsSe_3$ at 650 K (377 °C), $L_{U2} + HTM\text{-}AgAsSe_2 \leftrightarrow AgAs_3Se_5 + GeSe_2$ at 634 K (361 °C) and three eutectic ones: $L_{E1} \leftrightarrow Ag_8GeSe_6 + Ag_3AsSe_3 + HTM\text{-}AgAsSe_2$ at 640 K (367 °C), $L_{E2} \leftrightarrow Ag_8GeSe_6 + GeSe_2 + HTM\text{-}AgAsSe_2$ at 630 K (357 °C) and $L_{E3} \leftrightarrow GeSe_2 + As_2Se_3 + AgAs_3Se_5$ at 600 K (327 °C).

This work was performed as part of the effort to gather more data for a thermodynamic assessment of the Ag_2Se–

Table 7 Character, temperatures of invariant reactions and coordinates of invariant points in the quasi-ternary system Ag_2Se–$GeSe_2$–As_2Se_3

Invariant point	Process	T, K (T, °C)	Composition, mol.%		
			Ag_2Se	$GeSe_2$	As_2Se_3
e_1	$L \leftrightarrow AgAs_3Se_5 + As_2Se_3$	635 (362)	12	0	88
e_2	$L \leftrightarrow Ag_3AsSe_3 + HTM\text{-}AgAsSe_2$	655 (382)	65	0	35
e_3	$L \leftrightarrow Ag_8GeSe_6 + Ag_2Se$	1103 (830)	85	15	0
e_4	$L \leftrightarrow Ag_8GeSe_6 + GeSe_2$	843 (570)	44	56	0
e_5	$L \leftrightarrow Ag_8GeSe_6 + HTM\text{-}AgAsSe_2$	660 (387)	55.2	3.4	41.4
e_6	$L \leftrightarrow GeSe_2 + HTM\text{-}AgAsSe_2$	670 (397)	46	8	46
e_7	$L \leftrightarrow GeSe_2 + As_2Se_3$	618 (345)	0	20	80
p_1	$L + HTM\text{-}AgAsSe_2 \leftrightarrow AgAs_3Se_5$	644 (371)	18	0	82
p_2	$L + Ag_2Se \leftrightarrow Ag_3AsSe_3$	660 (387)	66	0	34
U_1	$L_{U1} + Ag_2Se \leftrightarrow Ag_8GeSe_6 + Ag_3AsSe_3$	650 (377)	65	3	32
U_2	$L_{U2} + HTM\text{-}AgAsSe_2 \leftrightarrow AgAs_3Se_5 + GeSe_2$	634 (361)	16	6	78
E_1	$L_{E1} \leftrightarrow Ag_8GeSe_6 + Ag_3AsSe_3 + HTM\text{-}AgAsSe_2$	640 (367)	62	2	36
E_2	$L_{E2} \leftrightarrow Ag_8GeSe_6 + GeSe_2 + HTM\text{-}AgAsSe_2$	630 (357)	51	8	41
E_3	$L_{E3} \leftrightarrow GeSe_2 + As_2Se_3 + AgAs_3Se_5$	600 (327)	4	12	84

$B^{IV}Se_2$–As_2Se_3 systems, where B^{IV}–Si, Ge, Sn, which is still in progress.

References

1. T. B. Massalski, Binary Alloy Phase Diagrams, ASM International, Materials Park, OH, 1990, Vols. **1–3**
2. G. Z. Vinogradova, Glass Formation and Phase Equilibria in Chalcogenide Systems. Binary and Ternary Systems, Nauka, Moscow, 1984
3. D. I. Bletskan, Crystalline and Glassy Semiconductors of Si, Ge, Sn and Their Alloys, Zakarpattia, Uzhgorod, 2004
4. M.A. Popesku, *Non-Crystalline Chalcogenides*. Kluwer Academie Publishers, New York, 2002.
5. A. Zakery, and S.R. Elliott, Optical Properties and Applications of Chalcogenide Glasses: A Review, *J. Non-Cryst. Solids*, 2003, **330**, p 1–12.
6. C. Goncalves, M. Kang, B. Sohn, G. Yin, J. Hu, D.T.H. Tan, and K. Richardson, New Candidate Multicomponent Chalcogenide Glasses for Supercontinuum Generation, *Appl. Sci*, 2018, **8**, p 2082.
7. O. Gorochov, Lescomposes Ag_8MX_6 (M = Si, Ge, Sn et X – S, Se, Te), *Bull. Soc. Chim. France*, 1968, **6**, p 2263–2275.
8. A.A. Movsun-zade, ZYu. Salaeva, and M.R. Allazov, The Ag–Ge–Se System, *Zhurn. Neorg. Khimii*, 1987, **32**(7), p 1705–1709.
9. O. P. Kokhan, Interaction in the Ag_2X – $B^{IV}X_2$ Systems (B^{IV} – Si, Ge, Sn; X – S, Se) and Properties of Compounds, Ph.D. (Chemistry) thesis, *Uzhgorod State Univ.*, Uzhgorod, 1996
10. I. Olekseyuk, O. Parasyuk, L. Piskach, G. Gorgut, O. Zmiy, O. Krykhovetz, L. Sysa, E. Kadykalo, O. Strok, O. Marchuk, and V. Halka, Quasi-Ternary Chalcogenide Systems, *Vezha*, 1999, Vol. **1**
11. D. Carre, R. Ollitrault-Fichet, and J. Flahaut, Structure de Ag_8GeSe_6 Beta, *Acta Cryst.*, 1980, **36**, p 245–249.
12. S.A. Tarasevich, Z.S. Medvedeva, I.S. Kovaleva, and L.I. Antonova, On Interaction in the Ternary System Ag–As–Se Along the Section Ag_2Se – As_2Se_3, *Zhurn. Neorg. Khimii*, 1972, **17**, p 1475–1478.
13. Y.V. Voroshilov, M.P. Golovey, and M.V. Potoriy, X-ray Investigations of the Compounds $AgAsSe_2$ and Ag_3AsSe_3, *Z. Kristallographie*, 1976, **21**(3), p 595–596.
14. D. Houphouet-Boigny, R. Ollitrault-Fichet, R. Eholie, and J. Flahaut, Sur le systeme Ag_2Se–As_2Se_3: Compose $AgAs_3Se_5$ et polimorphisme de $AgAsSe_2$, *CR Acad Sci Ser*, 1981, **292**(6), p 513–516.
15. K. Sakai, T. Koide, and T. Matsumoto, Silver Orthoselenoarsenite, *Acta Crystallogr.*, 1978, **34**, p 3326–3328.
16. O.S. Klymovych, O.F. Zmiy, L.D. Gulay, and T.A. Ostapyuk, Phase Diagram of the Ag_2Se–As_2Se_3 System and Crystal Structure of the $AgAs_3Se_5$ Compound, *Chem. Met. Alloys*, 2008, **1**, p 288–292.
17. O. Klymovych, I. Ivashchenko, I. Olekseyuk, O. Zmiy, and Z. Lavrynyuk, Quasi-Ternary System Cu_2Se–$GeSe_2$–As_2Se_3, *J. Phase Equilib. Diffus*, 2020, **41**(2), p 157–163.
18. P. Rahlfs, Über die kubischen Hochtemperaturmodifikationen der Sulfide und Telluride des Silbers und des einwertigen Kupfers, *Phase Transit*, 1992, **38**, p 127–220.
19. G. Dittmar, and H. Schäfer, The Crystal Structure of Germanium Dieselenide, *Acta Cryst.*, 1976, **32**, p 2726–2728.
20. A. Renninger, and B. Averbach, Crystalline Structures of As_2Se_3 and As_4Se_4, *Acta Cryst.*, 1973, **29**, p 1583–1589.
21. V.Y. Anosov, M.I. Ozerova, and Y.Y. Fialkov, *Fundamentals of Physico-chemical Analysis*. Nauka, Moscow, 1976.